This is a preprint, the final version is subject to change, of the American Mineralogist (MSA)
Cite as Authors (Year) Title. American Mineralogist, in press.
DOI: https://doi.org/10.2138/am-2018-6328

Revision 2

Surface-modified phillipsite-rich tuff from the Campania region (southern Italy) as a promising drug carrier: An Ibuprofen sodium salt trial

Mariano Mercurio[1*], Francesco Izzo[1], Alessio Langella[1], Celestino Grifa[1], Chiara Germinario[1], Aleksandra Daković[2], Paolo Aprea[3], Rossana Pasquino[3], Piergiulio Cappelletti[4], Fabio Sossio Graziano[4], Bruno de Gennaro[3]

[1]Dipartimento di Scienze e Tecnologie, Università degli Studi del Sannio, Via dei Mulini 59/A, 82100 Benevento, Italy

[2]Institute for Technology of Nuclear and Other Mineral Raw Materials, Franche d' Epere 86, 11000 Belgrade, Serbia

[3]DICMAPI, Università degli Studi di Napoli Federico II, Piazzale V. Tecchio 80, 80125 Naples, Italy

[4]Department of Earth Sciences, Environment and Resources, Federico II University, via Cinthia, 80126, Napoli, Italy

*Corresponding author: e-mail: mariano.mercurio@unisannio.it, ph. +390824305196, fax. +390824305199

ABSTRACT

The encapsulation and delivery of drugs often involves the use of expensive microporous materials, and we have investigated the potential for natural zeolites from the widespread volcanic formations of southern Italy as alternatives to these carriers. Surface-modified natural zeolites (SMNZs) with diverse micellar structures (patchy

and complete bilayers) were obtained by using different cationic surfactants (cetylpyridinium chloride (CP-Cl), benzalkonium chloride (BC-Cl), hexadecyltrimethylammonium chloride (HDTMA-Cl) and bromide (HDTMA-Br) with phillipsite-rich tuff from the Campania region (southern Italy). Loading and release kinetics tests of sodium Ibuprofen (IBU) were carried out with organo-phillipsite composites using Fourier-transform infrared spectroscopy (FTIR) and thermal analysis coupled with evolved gas analysis (EGA). Results from these tests were mathematically modeled to evaluate IBU adsorption and release mechanisms.

The maximum loaded amount of IBU was attained for organo-phillipsite modified with HDTMA-Br (PHB), which showed a complete bilayer micellar structure. Whenever a patchy bilayer micellar structure formed, the lowest adsorptions of IBU were observed. Equilibrium adsorption results were fit using Langmuir, Sips and Toth models. Pseudo first-order and pseudo second-order fits to the loading kinetic data provided significant Goodness of Fit. Good fits to the release kinetic data were obtained using first-order and Weibull equations, shedding new light on the release mechanism of IBU from phillipsite. The active amount of IBU on the modified zeolite surface was almost totally available for pharmaceutical purposes.

Keywords: phillipsite; Neapolitan Yellow Tuff; Ibuprofen sodium salt; functionalization; SMNZ; carrier; drug delivery; SIPS model; TOTH model.

INTRODUCTION

This is a preprint, the final version is subject to change, of the American Mineralogist (MSA)
Cite as Authors (Year) Title. American Mineralogist, in press.
DOI: https://doi.org/10.2138/am-2018-6328

Recent research has demonstrated that natural and surface-modified zeolites containing cationic surfactants are selective towards some pharmacological molecules (i.e., diclofenac sodium, diclofenac diethylamine, and Ibuprofen). Available data suggest that zeolites represent a low cost and easily accessible natural excipient that can be used in biomedicine as carriers for drug delivery (Cerri et al. 2004, 2016, Krajišnik et al. 2013b, 2015, 2010a, 2010b, 2011, 2013a; Cappelletti et al. 2017; de Gennaro et al. 2015, 2016; Janićijević et al. 2015; Marković et al. 2016, 2017; Pasquino et al. 2016; Serri et al. 2016, 2017). Based on the premise that such natural carriers are non-toxic (Mercurio et al. 2012, 2016b; Krajišnik et al. 2013b; Cerri et al. 2016), several aspects of their performance should be clarified before modified zeolites can be used on an industrial scale. In order to evaluate their functional therapeutic performance, it is particularly important to expand the data for a breadth of different systems such as zeolite vs. surfactant vs. active substance. Careful evaluation of loading and release performances under controlled conditions is also required (Krajišnik et al. 2015, 2010a, 2010b, 2011, 2013a, 2013b, de Gennaro et al. 2015, 2016, 2017; Janićijević et al. 2015; Marković et al. 2016, 2017; Pasquino et al. 2016; Serri et al. 2016, 2017; Izzo et al. 2017). Several recent studies have documented the efficacy of zeolites as pharmacological carriers. Serri et al. (2017) demonstrated that granulate could be formed using a functionalized natural clinoptilolite, suitable for the release of sodium diclofenac. Krajišnik et al. (2016) demonstrated that non-steroidal anti-inflammatory drugs (NSAID), for example IBU, benefit particularly from use with therapeutic devices providing prolonged release, such as clinoptilolite-rich carriers. For loading purposes, Krajišnik et al. (2016) used clinoptilolite modified with two surfactants

(cetylpyridinium chloride and benzalkonium chloride) at different concentrations, and their results showed that different adsorbed amounts of IBU depended on the type and/or the amount of surfactant used to functionalize the zeolite-rich carrier. In *vitro* release tests also demonstrated that IBU was released from the composite material for up to eight hours, as illustrated by mathematical models Bhaskar (Bhaskar et al. 1986) and Higuchi (Higuchi 1963). Krajišnik et al. (2016) hypothesized that the adsorption process involved hydrophobic-hydrophilic interactions between the drug molecules and the surfactants on the zeolite surface.

In order to meet the demand of the pharmaceutical industry searching for new and inexpensive carriers for the encapsulation and delivery of drugs (Tan et al. 2013), we investigated natural and widespread phillipsite-rich rock from southern Italy (Campania region) as alternatives to the usual expensive prepared mesoporous materials. This geomaterial, widely occurring in the Neapolitan Yellow Tuff (NYT) Formation and the Campanian Ignimbrite (CI) Formation, has been studied in detail (de Gennaro et al. 1992, 1995, 1999, 2000a; Colella et al. 1998, 2013, 2017; Langella et al. 2002, 2013; Cappelletti et al. 2003; Calcaterra et al. 2004; Buondonno et al. 2008; Morra et al. 2010), and existing data support applications in the areas of cation exchange (Pansini et al. 1996; Colella et al. 1998; Gatta et al. 2015), animal feeding (Mercurio et al. 2012, 2016b), oenotechnical (Mercurio et al. 2010, 2014, 2016a), soil remediation (Coppola et al. 2003), production of lightweight aggregates (de Gennaro et al. 2004, 2005, 2007, 2008; Dondi et al. 2016), and ceramic manufacturing (de Gennaro et al. 2003; Cappelletti et al. 2011).

This is a preprint, the final version is subject to change, of the American Mineralogist (MSA)
Cite as Authors (Year) Title. American Mineralogist, in press.
DOI: https://doi.org/10.2138/am-2018-6328

Application of natural zeolites in the pharmaceutical field requires evaluation of the performance of functionalized zeolites as carriers for drug delivery. Modification of the zeolite surface was performed in our studies using four different surfactants (cetylpyridinium chloride, benzalkonium chloride, hexadecyltrimethylammonium chloride and bromide) at a concentration equal to 200% of the external cation exchange capacity (ECEC) of the zeolite. The amount of surfactant was chosen based on published results (Li and Bowman 1997; de Gennaro et al. 2016; Cappelletti et al. 2017) that demonstrated that this concentration guarantees the almost complete formation of a bilayer of the surfactants on the zeolite surface.

In order to clarify the properties of this specific phillipsite-IBU composite material, equilibrium isotherms as well as IBU loading and release kinetics were measured. Basic characterization of the composite material was obtained using thermal analysis (STA coupled with EGA) and FT-IR spectroscopy.

MATERIALS

A phillipsite-rich tuff from the Campania Region (southern Italy) and four cationic surfactants were selected for the preparation of surfactant modified natural zeolites (SMNZs) and were used for subsequent IBU sodium loading and release tests. Mineralogical and technological characterization of the natural zeolite-rich material has been reported by Cappelletti et al. (2017) and is only briefly summarized here. NYT phillipsite-rich rocks from Marano (Savanelli quarry, Naples, Italy; hereafter PHI_SAV) contain about 70 wt.% phillipsite with minor chabazite (~5 wt.%) and analcime (~3 wt.%) (de' Gennaro et al. 2000b). This phillipsite from the PHI_SAV

sample has a low Si/Al ratio (approximately 2.5) and it is characterized by a high K^+ content, which reflects the typical composition of trachytic rocks from Campi Flegrei (southern Italy) (Morra et al. 2010). It contains subordinate amounts of Ca^{2+} and Na^+. The experimental ECEC value (0.144 mEq/g) was evaluated using the method suggested by de Gennaro et al.(2014), which involves contacting a zeolite sample (2.5 g) with 10 mL of 20-mM surfactant solution in a 50-mL polyallomer centrifuge tube, shaking at 100 rpm for 24 h at 25 °C. The sample was then centrifuged and the supernatant analyzed for the anion concentration by HPLC.

Leaching tests confirmed that the available contents of heavy metals such as Ni, As, Cd and Pb were all below 20 mg/kg, confirming the correlation with the total amount of these elements in the whole rock (Mercurio et al. 2012).

PHI_SAV was surface modified using cetylpyridinium chloride (CP-Cl), benzalkonium chloride (BC-Cl), hexadecyltrimethylammonium chloride (HDTMA-Cl) and bromide (HDTMA-Br). The resulting SMNZs were labeled as PCC, PBC, PHC and PHB, respectively. Anion exchange capacity (AEC) values for these were ~0.09 mEq/g for PBC and PC, and ~0.110 mEq/g and 0.140 mEq/g for PHC and PHB. These results are consistent with the different micellar structure (patchy and complete bilayer) obtained using different surfactant molecules (Cappelletti et al., 2017).

These organo-phillipsite composites were used for loading and release tests of sodium IBU. Chemical characteristics of surfactants and IBU are presented in Figures 1 and 2.

METHODS

SMNZs preparation

In order to obtain SMNZs for the IBU loading tests, a suspension containing PHI_SAV and each of the selected surfactants, having an initial concentration equivalent to 200% of the ECEC, was prepared. The suspension was mixed at 3,000 rpm using a FALC AT-M 20 stirrer at ~ 50 °C for ~ six hours, with a solid to liquid (S/L) ratio of 1/40. The suspensions were then filtered and the obtained SMNZs were washed with ultrapure water to remove the unnecessary surfactant and were then dried at room temperature for 24 hours.

Drug loading tests

Maximum IBU adsorption capacities of SMNZs were determined by means of equilibrium and kinetics adsorption tests. The pH of each suspension was adjusted to 7.4 with a sodium tetraborate buffer solution (CAS No. [1303-96-4]) as this pH value allows the IBU sodic salt to remain in its ionic form (Krajišnik et al. 2015; Oh et al. 2016).

For the equilibrium adsorption measurements, 100 mg of each SMNZ were treated with 20 mL of IBU solution, having concentrations ranging between 50 and 1000 mg/L, and continuously stirred in 25 mL Nalgene centrifuge tubes at room temperature. After four hours (sufficient time to attain equilibrium based on the kinetic tests), samples were centrifuged to separate solid from liquid and the supernatant was analyzed using an AquaMate UV-VIS spectrophotometer. The IBU calibration curve (R^2=0.999) was obtained using the adsorption band at 224 nm, in accordance with (Sena et al. 2007; Gondalia et al. 2010; Joshi et al. 2011). Each measurement was made in triplicate.

This is a preprint, the final version is subject to change, of the American Mineralogist (MSA)
Cite as Authors (Year) Title. American Mineralogist, in press.
DOI: https://doi.org/10.2138/am-2018-6328

Kinetic studies were carried out in batch experiments at room temperature and under continuous stirring, by shaking 100 mg of each sample with 20 mL of IBU solution (400 mg/L). To avoid variation of this solution/SMNZ ratio the mixture was placed into 25 mL high density polyethylene centrifuge tubes. A test tube was withdrawn (after 5', 10', 15', 30', 60', 90'…240), centrifuged, and the non-adsorbed amount of IBU was determined in the supernatant.

Drug release tests

IBU *in vitro* release experiments were carried out using IBU-loaded SMNZs dispersed in simulated intestinal fluid (SIF), prepared as described in the United States Pharmacopoeia 25 Ed. and later editions (USP-NF 2002, 2003). 15 mg of IBU-loaded SMNZs were added to 10 mL of SIF and placed in a thermostatic bath at 37 °C under continuous stirring (100 rpm). Samples were kept in the thermostatic bath until the released amount of the drug reached a plateau. The IBU-loaded SMNZ/SIF ratio was chosen in order to ensure sink conditions. 5 mL aliquots of supernatant were withdrawn at fixed interval times (30 min), centrifuged at 9,000 rpm (room temperature, 5 min), and replaced by the same volume of fresh medium. IBU was quantified by spectrophotometric assay (Aquamate UNICAM) at 224 nm. Experiments were run in triplicate.

Mathematical modeling

To evaluate IBU adsorption and release mechanisms of SMNZs, adsorption isotherms and kinetic measurements were fit using several mathematical models proposed in the

This is a preprint, the final version is subject to change, of the American Mineralogist (MSA)
Cite as Authors (Year) Title. American Mineralogist, in press.
DOI: https://doi.org/10.2138/am-2018-6328

literature (Hinz 2001; Ho 2004, 2006; Ho et al. 2005; Limousin et al. 2007; Dash et al. 2010; Foo and Hameed 2010; Wang and Peng 2010; Chen 2013; Yadav et al. 2013). Fit parameters were determined by non-linear regression using the Generalized Reduced Gradient algorithm (Gabriele and Ragsdell 1977), based on the assumption that non-linear regression provides the best fit results (Ho et al. 2005; Lin and Wang 2009; Chen 2013; Markandeya and Kisku 2015).

Model fit and applicability were evaluated by considering determination coefficients (R^2), as well as other statistical methods for non-linear regression (Costa et al. 2003; Spiess and Neumeyer 2010) such as the Akaike Information Criterion (AIC) (1) and the Bayesian Information Criterion (BIC) (2). These methods take into account the number of parameters of the mathematical model and the number of experimental data and can be expressed as follows:

$$AIC = 2p - 2\ln(L) \quad ; \tag{1}$$

$$BIC = p\ln(n) - 2\ln(L)\,, \tag{2}$$

where p is the number of parameters and n is the sample size. ln (L), the maximum log-likelihood of the estimated model (Spiess and Neumeyer 2010), was calculated as follows: $ln(L) = 0.5 * [-N * (ln2\pi + 1 - lnN + ln\sum_{i=1}^{n} x_i^2)]$, where x_i are the residuals from the nonlinear least squares fit and N = the number of residuals.

Thermal analyses

Thermal analysis (thermogravimetry and differential scanning calorimetry, TG/DSC) was performed on phillipsite-rich material, cationic surfactants, IBU, SMNZs and IBU-loaded SMNZs using a NETZSCH STA 449 F3 Jupiter instrument with alumina crucibles. Samples were heated from room temperature to 1050 °C at a heating rate of 10 °C/min in an ultra-pure air atmosphere (N_2/O_2 = 80/20; flow 60 mL/min). EGA were carried out by FTIR with a BRUKER Tensor 27 instrument, coupled to the STA 449 F3 instrument by a transfer line heated to 200 °C.
Netzsch Proteus 6.1.0 (NETZSCH-Gerätebau GmbH) and Opus 7.2 (Bruker Optics GmbH) software packages were used for data analysis.

FTIR

The phillipsite-rich material, cationic surfactants, IBU, SMNZs and IBU-loaded SMNZs were analyzed using a Bruker Alpha FTIR spectrometer in attenuated total reflectance (ATR)-mode with 128 scans at a spectral resolution of 4 cm^{-1} in the spectral range of 400-4000 cm^{-1}. Spectra were analyzed with Opus 7.2 software (Bruker Optics GmbH).

RESULTS AND DISCUSSION

Characterization of SMNZs

FTIR spectroscopy

The infrared spectrum of PHI_SAV shows the typical absorption bands of zeolite-rich tuffs (Cappelletti et al. 2017), including absorption bands associated with internal and external framework vibrations of primary building units (PBUs) and secondary

building units (SBUs) of zeolites (Karge 2001; Byrappa and Kumar 2007; Mozgawa et al. 2011). A strong band at ~1000 cm^{-1} (Table 1 and Fig. 3) was assigned to asymmetric stretching Si-O vibrations. Bands at ~780 and ~719 cm^{-1} were assigned to asymmetric and symmetric stretching T-O-T vibrations, respectively, and the remaining bands are generally referred to bending vibrations characteristic for silicates, also occurring in the sample, such as pyroxene (3.3 wt.%), K-feldspar (13.3 wt.%) and traces of mica. The weak, broad band at ~ 3419 cm^{-1} and the band at ~1638 cm^{-1} suggest the presence of hydrogen-bonded H_2O molecules.

Moreover, a very weak broad band at ~1456 cm^{-1} could indicate traces of carbonate minerals (C-O asymmetric stretching in the carbonate ion).

IR vibrations associated with exchangeable cations usually occur in the far-IR region (200-50 cm^{-1}) (Karge 2001), and any structural modification caused by external cation substitution with cationic surfactants could not be detected by mid-IR spectroscopy.

On the other hand, FTIR spectra of SMNZs and IBU-loaded SMNZs can be clearly distinguished from those of the starting materials by the presence of absorption bands in the spectral range 3000-2800 cm^{-1} (Table 1; Fig. 3) (Barczyk et al. 2014), which correspond to the strong bands (C-H stretching vibrations) observed both in surfactants and IBU (Figures 1 and 2). These organic compounds also share two very weak bands at ~1487 cm^{-1} and ~1468 cm^{-1} (C-H bending vibrations). However, IBU-loaded SMNZs show increased intensity of C-H stretching vibrations (Krajišnik et al. 2010b, 2015), as well as the occurrence of additional bands at ~1578 cm^{-1} and ~1380 cm^{-1} (Table 1; Fig. 3) attributable to asymmetric and symmetric stretching vibrations in carboxylate ions (Ambrogi et al. 2001; Wray et al. 2011).

This is a preprint, the final version is subject to change, of the American Mineralogist (MSA)
Cite as Authors (Year) Title. American Mineralogist, in press.
DOI: https://doi.org/10.2138/am-2018-6328

250

251 *STA coupled with FT-IR/EGA*

252 Thermal analysis has been widely used in the characterization of natural zeolites and
253 their modified forms (Sullivan et al. 1997; Bish and Carey 2001; Langella et al. 2003;
254 Krajišnik et al. 2011, 2013a, 2013b; de Gennaro et al. 2016; Marković et al. 2017). So-
255 called "zeolitic water" is found in the open cavities (channels and cages) of zeolites
256 (Coombs et al. 1997), where it can move more-or-less freely through the
257 interconnected cavities (Bish and Carey 2001; Langella et al. 2003). The phillipsite-
258 rich starting material shows the typical thermal behavior of a zeolite with a high kinetic
259 pore diameter (Bish and Carey 2001; Langella et al. 2003), as much of the weight loss
260 occurs below 250 °C with the maximum dehydration rate at ~ 176 °C (Fig. 4).
261 Dehydration continued gradually to ~ 550 °C, likely due to the presence of other
262 natural zeolites with lower kinetic diameters such as chabazite and minor analcime as
263 well as hydroxilated phases (micas). Cumulatively, the "zeolitic" H_2O evolving over
264 the 40-550 °C range is ~10 wt.%. This H_2O content is consistent with the high K^+
265 content of the zeolites in the tuff. The presence of large monovalent cations, such as K^+,
266 generally results in moderate or low H_2O contents (Bish 1984, 1988; Kranz et al. 1989;
267 Carey and Bish 1996; Fialips et al. 2005; Esposito et al. 2015).
268 H_2O evolved during dehydration was detected via FTIR/EGA (Fig. 4), along with a
269 weak emission of CO_2 attributable to the decomposition of calcite in the 550-800 °C
270 thermal range.
271 The thermal behavior of SMNZs and IBU-loaded SMNZs is mainly characterized by
272 the occurrence of two principal processes (Table 2). The first, occurring below 200 °C,

is related to dehydration of the zeolitic component, and decomposition of cationic surfactants was not significant in this temperature range (Fig. 4). The second process (>200 °C) is linked to decomposition and subsequent combustion of surfactants (SMNZs) and IBU (IBU-loaded SMNZs) (Table 2; Figs 1 and 2). Thus the total mass loss for IBU-loaded SMNZs is greater than the mass loss for the starting material and the SMNZs before drug adsorption (Table 2).

These results could attest the effective functionalization of zeolite and subsequent drug loading although, it requires a further validation by technological performance.

Technological performance of the phillipsite-IBU composite material

Equilibrium isotherms

Table 3 and Figure 5 report the results of equilibrium adsorption measurements fit using three mathematical models, Langmuir (Fig. 5a) (Langmuir 1916), Sips (also called Langmuir-Freundlich, Fig. 5b), and Toth (Fig. 5c) equations.

The shape of the curves shows that the plateau, i.e., the maximum drug adsorption, was reached for the initial IBU concentration of 400 mg/L, regardless of the type of surfactant. Moreover, the maximum loaded amount was attained for the PHB (~29 mg/g), in agreement with complete bilayer formation, whereas lower adsorption was achieved for PBC and PCC (21.2 mg/g) where the two surfactants formed only a patchy bilayer at the zeolitic surface. The latter are in agreement with Cappelletti et al. (2017), who emphasized the effects of the counterions on micellar structure formation. The same behavior was also recorded for PHC, although it achieved a higher IBU loaded amount. This may indicate that, for its benzene ring-free structure (different

296 from benzalkonium and cetylpyridinium), the HDTMA-Cl can form a more
297 homogeneous patchy bilayer than the other two chlorinated surfactants, as found in
298 previous research (Cappelletti et al., 2017).
299 The Langmuir adsorption isotherm model is commonly used to fit the performance of
300 different bio-mineral adsorbents such as SMNZs (Li et al. 1998, 1999; Krajišnik et al.
301 2010a; Wang and Peng 2010; Cappelletti et al. 2017; de Gennaro et al. 2016; Marković
302 et al. 2017) and other geomaterials (Campbell and Davies 1995; Li and Bowman 1997,
303 1998, 2001; Janićijević et al. 2015), although it was originally developed to describe
304 gas-solid-phase adsorption onto activated carbon (Langmuir 1916; Foo and Hameed
305 2010). On the other hand, the Sips (1948) and Toth (1971) models were developed to
306 improve fits based on Langmuir isotherms (Hinz 2001; Limousin et al. 2007; Foo and
307 Hameed 2010).
308 The Langmuir (equation 3), Sips (equation 4), and Toth (equation 5) equations can be
309 expressed as follows:
310

311 $$S = S_m \frac{KC_e}{1+KC_e}, \quad (3)$$

312

313 $$S = S_m \frac{(KC_e)^n}{1+(KC_e)^n}, \text{ and} \quad (4)$$

314

315 $$S = S_m \frac{KC_e}{[1+(KC_e)^n]^{\frac{1}{n}}}, \quad (5)$$

316 where S is the amount of solute adsorbed by the solid at equilibrium conditions (mg/g);
317 C_e is the concentration of solute in solution after equilibrium (mg/L); S_m is the

maximum adsorption capacity at equilibrium (mg/g), *K* (L/mg) is the adsorption intensity, a constant related to binding energy, and *n* is a fitting parameter related to heterogeneity of the system. If *n* =1, the Sips and Toth equations become a simple Langmuir equation.

The Sips and Toth models generally provided improved Goodness-Of-Fit (GOF) values observed as a reduction of AIC and BIC values, as well as an increase in the determination coefficient R^2 (Table 3). Maximum IBU adsorption capacities (S_m) of 22.0 mg/g, 20.4 mg/g, and 20.4 mg/g was calculated for sample PCC according to the Langmuir, Sips, and Toth isotherm equations, respectively (Table 3). Both the Sips (1948) and Toth (1971) provided best fits (R^2 = 0.987; AIC = 23.1; BIC = 22.9) for PCC, but no significant differences were found between these three models for IBU adsorption by PBC (Table 3).

Greater maximum adsorption capacities were obtained for PHC and PHB compared with PCC and PBC, and the Toth equation provided the best fit to the data (Table 3 and Fig. 5), particularly for PHB.

The Toth fit parameters yield an amount of adsorbed IBU of 24.4 mg/g for PHC and 28.8 mg/g for PHB. The better performance of PHB can be explained by the tendency of this composite to form a more compact bilayer sheet micelle due to the presence of a Br counterion (Li and Bowman 1997; Cappelletti et al. 2017; de Gennaro et al. 2016).

The general improvement of the GOF with the Sips and Toth equations instead of the Langmuir can be explained by taking into account the theoretical basis of the Langmuir isotherm model (Langmuir 1916; Limousin et al. 2007; Foo and Hameed 2010). The Langmuir model is strictly intended for materials where sorption mechanisms are fully

associated with adsorption processes. The model is therefore inappropriate for SMNZs where sorption of NSAIDs is controlled by multiple mechanisms, including both external anionic exchange and partition into the hydrophobic portion of the micelle (Krajišnik et al. 2010a, 2010b, 2011, 2013a, 2013b, 2015; de Gennaro et al. 2015; Marković et al. 2016; Pasquino et al. 2016; Serri et al. 2017). In case of multiple sorption mechanism, although the adsorption mechanism always predominates (de Gennaro et al. 2015; Krajišnik et al. 2015), partition may influence the sorption of IBU by SMNZs, especially when IBU molecules can change their ionic form (e.g. by pH variations). Thus, from a mathematical point of view, the Sips or Toth equations fit the adsorption data better than the Langmuir model and they provide a well-defined equilibrium asymptotic plateau, useful for the identification of the real maximum adsorption capacity of SMNZs. In this way, equilibrium isotherm modeling can be used to optimize the appropriate initial concentration of IBU for kinetic experiments.

In vitro IBU loading and release tests

As mentioned above, the initial concentration of the IBU solution for the kinetic tests was 400 mg/L; at this concentration, complete saturation of the host composite material (SMNZ) is guaranteed, as suggested by the model equilibrium isotherms, and greater initial concentrations of the drug do not provide further IBU uptake. Figure 6 highlights the rapid rate of the loading process, and > 90% of IBU was loaded onto the SMNZs after 30 min, except for PBC which required ~120 min. Comparison of kinetic curves reveals that the maximum amount of loaded IBU was reached for PHC and PHB (26.8 and 28.1 mg/g, respectively). The latter case illustrates that a compact

This is a preprint, the final version is subject to change, of the American Mineralogist (MSA)
Cite as Authors (Year) Title. American Mineralogist, in press.
DOI: https://doi.org/10.2138/am-2018-6328

bilayer is not an indication of the best loading, as it can create a "crowding" of anionic sites that are not all available for drug adsorption due to the larger size of IBU when compared with the Br ion. The maximum loaded amounts for PBC and PCC are still comparable (20.0 and 19.2 mg/g, respectively), confirming the similar behavior of SMNZs modified with these two surfactants. Lastly, the similarity of the values (Table 4, in mEq/g) of the maximum amounts of drug loaded onto SMNZs and their respective AECs (with the exception of PHB, as reported above) strongly suggests that anion exchange is the primary mechanism involved in the loading of IBU on SMNZs. As often reported in the literature (Bowman 2003; de Gennaro et al. 2015; Serri et al. 2016), the drug adsorption kinetics of SMNZs generally follow pseudo-first order (PFO) (6) (Ho 2004) and pseudo-second order models (PSO) (7) (Ho 2006) . These models can be written as follows:

$$Q_t = Q_0(1 - e^{-K_1 t}) \quad \text{and} \tag{6}$$

$$Q_t = \frac{K_2 Q_0^2 t}{1 + K_2 Q_0 t}, \tag{7}$$

where Q_t is the amount of IBU loaded in SMNZ (mg/g) as a function of time t (min), Q_0 is the drug concentration at equilibrium, and K_1 (min^{-1}) and K_2 ($g/mg^{-1}\ min^{-1}$) are the pseudo-first and the pseudo-second order constants, respectively.

Non-linear regression validated both of these models (Table 4 and Fig. 6), although the best fit was obtained with the pseudo-second order model, consistent with previous

This is a preprint, the final version is subject to change, of the American Mineralogist (MSA)
Cite as Authors (Year) Title. American Mineralogist, in press.
DOI: https://doi.org/10.2138/am-2018-6328

research on NSAIDs loaded on SMNZs (de Gennaro et al. 2015). Maximum adsorption capacities were 19.3 mg/g for PCC, 20.9 mg/g for PBC, 26.4 mg/g for PHC, and 27.9 mg/g for PHB (calculated using the PSO model). Once again, the highest IBU adsorption was achieved by PHB and PHC, whereas the amount of IBU adsorbed by PCC and PBC were lower, although quite similar.

IBU-release kinetics, rapid and practically complete (> 95%) for all the SMNZs, were fit using several mathematical models reported in the literature (Costa and Sousa Lobo 2001; Costa et al. 2003; Dash et al. 2010; Yadav et al. 2013), but the best fit was obtained using the first-order equation (8) and the Weibull equation (9), expressed as follows:

$$M_t = M_0(1 - e^{-K_1 t}) \text{ and} \quad (8)$$

$$M_t = M_0\left[1 - e^{-\left(\frac{t-T_i}{a}\right)^b}\right], \quad (9)$$

where M_t is the amount of IBU released by SMNZ (mg/g) as a function of time t (min), M_0 is the drug concentration at equilibrium (mg/g), K_1 is the first-order constant (min^{-1}), T_i is the lag time (usually zero), a defines the time scale of the process (min), and b is a parameter describing the shape of the dissolution profile. In particular, the curve is exponential when $b = 1$, the profile becomes sigmoidal with a turning point after an upward curvature if $b > 1$, and the profile is parabolic with a steeper initial slope when $b < 1$.

Table 5 reports the parameters of these two models fitted by non-linear regression, and the dissolution profiles are shown in Figure 7, which shows that 50-60% of IBU was released by all samples in the first 30 min and 85-90 % released within the first hour. Nevertheless, slower drug release from the SMNZs occurred up to 5 hours, with none of them achieving 100% release (Table 5).

Although the Weibull model is often useful for comparing dissolution profiles of matrix-type drug delivery (Costa and Sousa Lobo 2001), providing good fitting results (Costa et al. 2003), it represents an empirical model without any kinetic basis. The Weibull model can therefore not be used to adequately describe the dissolution rate of a drug or to establish effective correlations between *in vitro* and *in vivo* experiments (Costa and Sousa Lobo 2001).

Alternatively, a first-order kinetic equation may better describe dissolution profiles of IBU-loaded SMNZs, as the drug release appears to be proportional to the IBU remaining in the composites (Yadav et al. 2013). In particular, much of the released NSAID may be related to the amount of IBU adsorbed on the surface of SMNZs, whereas minor amounts of IBU located in the hydrophobic chains of micelles would be more slowly released due to diffusion processes (Pasquino et al. 2016).

IMPLICATIONS

One of the most important implications of this research is the possible use of low-cost and largely available natural zeolites in advanced technological sectors such as biomedicine. Our research has demonstrated that a phillipsite-rich rock is a good drug carrier, comparable to clinoptilolite-bearing rock carriers. Our results provide added

value to the southern Italian zeolitite deposits, representing a by-product of the building stone industry that is currently disposed in landfills. However, due to the natural variability of this resource, careful characterization of production batches is mandatory.

Experimental results provide evidence that this material, properly surface modified by long-chain surfactants, is an excellent carrier of NSAIDs. Appropriate pharmaceutical preparations for oral use can be developed, possibly as granulates or as dispersions in order to increase the amount of the released drug. This application is supported by laboratory data that have shown the prompt release of a pain-killing drug within the first 30-50 min, thereby making these natural materials suitable for providing rapid palliative effects to the patient. It should be remarked however that the formulation of a composite system able to provide a sustained- in time drug release is required by pharmacologists. The IBU-phillipsite composite material investigated in the present research provided a slow release of a small amount of drug (5-10 %). Further investigation is required to understand if this low amount is significant of pharmacological point of view.

The functionalized phillipsite-rich rock may have other important applications in environmental fields (Hailu et al. 2017) such as the absorption/removal of pharmaceuticals from ground or surface waters, a rather growing problem which has yet to find a satisfactorily solution (Larsson 2014; Płuciennik-Koropczuk 2014).

ACKNOWLEDGMENTS

This work was carried out with the financial support of MIUR (Ministero dell'Istruzione, dell'Università e della Ricerca) Progetti di Ricerca di Interesse Nazionale (PRIN 2010). Authors wish to thank K. Putirka and two anonymous referees for their suggestions, which deeply improved the manuscript. The Authors are also in debt with L. Campbell and D.L. Bish for the invaluable contribution to the clarity of the manuscript.

REFERENCES CITED

Ambrogi, V., Fardella, G., Grandolini, G., and Perioli, L. (2001) Intercalation compounds of hydrotalcite-like anionic clays with antiinflammatory agents - I. Intercalation and in vitro release of ibuprofen. International Journal of Pharmaceutics, 220, 23–32.

Barczyk, K., Mozgawa, W., and Król, M. (2014) Studies of anions sorption on natural zeolites. Spectrochimica Acta Part A: Molecular and Biomolecular Spectroscopy, 133, 876–882.

Bhaskar, R., Murthy, R.S.R., Miglani, B.D., and Viswanathan, K. (1986) Novel method to evaluate diffusion controlled release of drug from resinate. International Journal of Pharmaceutics, 28, 59–66.

Bish, D.L. (1984) Effects of exchangeable cation composition on the thermal expansion/contraction of clinoptilolite. Clays and Clay Minerals, 32, 444–452.

Bish, D.L. (1988) Effects of composition on the dehydration behavior of clinoptilolite and heulandite. In Occurrence, Properties and Utilization of Natural Zeolites pp. 565–576. Akadémiai Kiadó, Budapest.

Bish, D.L., and Carey, J.W. (2001) Thermal Behavior of Natural Zeolites. Reviews in Mineralogy and Geochemistry, 45, 403 LP-452.

Bowman, R.S. (2003) Applications of surfactant-modified zeolites to environmental remediation. Microporous and Mesoporous Materials, 61, 43–56.

Buondonno, A., Colella, A., Coppola, E., de Gennaro, M., Grilli, E., Langella, A., and Rubino, M. (2008) Distribution of Al, Ca, Fe and Mg in weathering extracts from Campanian Ignimbrite (yellow facies). Studies in Surface Science and Catalysis, 174, 525–528.

Byrappa, K., and Kumar, B.V.S. (2007) Characterization of zeolites by infrared spectroscopy. Asian Journal of Chemistry, 19, 4933–4935.

Calcaterra, D., Cappelletti, P., Langella, A., Colella, A., and de Gennaro, M. (2004) The ornamental stones of Caserta province: the Campanian Ignimbrite in the medieval architecture of Casertavecchia. Journal of Cultural Heritage, 5, 137–148.

Campbell, L.S., and Davies, B.E. (1995) Soil sorption of caesium modelled by the Langmuir and Freundlich isotherm equations. Applied Geochemistry, 10, 715–723.

Cappelletti, P., Cerri, G., Colella, A., de'Gennaro, M., Langella, A., Perrotta, A., and Scarpati, C. (2003) Post-eruptive processes in the Campanian Ignimbrite. Mineralogy and Petrology, 79, 79–97.

Cappelletti, P., Rapisardo, G., De Gennaro, B., Colella, A., Langella, A., Graziano, S.F., Bish, D.L., and De Gennaro, M. (2011) Immobilization of Cs and Sr in aluminosilicate matrices derived from natural zeolites. Journal of Nuclear Materials, 414, 451–457.

500 Cappelletti, P., Colella, A., Langella, A., Mercurio, M., Catalanotti, L., Monetti, V.,
501 and de Gennaro, B. (2017) Use of surface modified natural zeolite (SMNZ) in
502 pharmaceutical preparations Part 1. Mineralogical and technological
503 characterization of some industrial zeolite-rich rocks. Microporous and
504 Mesoporous Materials, 250, 232–244.
505 Carey, J.W., and Bish, D.L. (1996) Equilibrium in the clinoptilolite-H2O system.
506 American Mineralogist.
507 Cerri, G., de Gennaro, M., Bonferoni, M.C., and Caramella, C. (2004) Zeolites in
508 biomedical application: Zn-exchanged clinoptilolite-rich rock as active carrier for
509 antibiotics in anti-acne topical therapy. Applied Clay Science, 27, 141–150.
510 Cerri, G., Farina, M., Brundu, A., Daković, A., Giunchedi, P., Gavini, E., and Rassu, G.
511 (2016) Natural zeolites for pharmaceutical formulations: Preparation and
512 evaluation of a clinoptilolite-based material. Microporous and Mesoporous
513 Materials, 223, 58–67.
514 Chen, C. (2013) Evaluation of Equilibrium Sorption Isotherm Equations. The Open
515 Chemical Engineering Journal, 7, 24–44.
516 Colella, A., Calcaterra, D., Cappelletti, P., Di Benedetto, C., Langella, A., Papa, L.,
517 Perrotta, A., Scarpati, C., and de Gennaro, M. (2013) Il Tufo Giallo Napoletano.
518 In Le pietre storiche della Campania dall'oblio alla riscoperta pp. 129–154.
519 Luciano Editore.
520 Colella, A., Di Benedetto, C., Calcaterra, D., Cappelletti, P., D'Amore, M., Di Martire,
521 D., Graziano, S.F., Papa, L., de Gennaro, M., and Langella, A. (2017) The
522 Neapolitan Yellow Tuff: An outstanding example of heterogeneity. Construction

523 and Building Materials, 136, 361–373.
524 Colella, C., de Gennaro, M., Langella, A., and Pansini, M. (1998) Evaluation of
525 Natural Phillipsite and Chabaziteas Cation Exchangers for Copper and Zinc.
526 Separation Science and Technology, 33, 467–481.
527 Coombs, D.S., Alberti, A., Armbruster, T., Artioli, G., Colella, C., Galli, E., Grice, J.D.,
528 Liebau, F., Mandarino, J.A., Minato, H., and others (1997) Recommended
529 nomenclature for zeolite minerals: report of the subcommittee on zeolites of the
530 International Mineralogical Association, Commission on new Minerals and
531 Mineral names. Canadian Mineralogist, 35, 1571–1606.
532 Coppola, E., Battaglia, G., Bucci, M., Ceglie, D., Colella, A., Langella, A., Boundonno,
533 A., and Colella, C. (2003) Remediation of Cd- and Pb-polluted soil by treatment
534 with organo-zeolite conditioner. Clays and Clay Minerals, 51, 609–615.
535 Costa, F.O., Sousa, J.J.S., Pais, A.A.C.C., and Formosinho, S.J. (2003) Comparison of
536 dissolution profiles of Ibuprofen pellets. Journal of Controlled Release, 89, 199–
537 212.
538 Costa, P., and Sousa Lobo, J.M. (2001) Modeling and comparison of dissolution
539 profiles. European Journal of Pharmaceutical Sciences.
540 Dash, S., Murthy, P.N., Nath, L., and Chowdhury, P. (2010) Kinetic modeling on drug
541 release from controlled drug delivery systems. Acta poloniae pharmaceutica, 67,
542 217–23.
543 de Gennaro, B., Catalanotti, L., Bowman, R.S., and Mercurio, M. (2014) Anion
544 exchange selectivity of surfactant modified clinoptilolite-rich tuff for
545 environmental remediation. Journal of Colloid and Interface Science, 430, 178–

183.

de Gennaro, B., Catalanotti, L., Cappelletti, P., Langella, A., Mercurio, M., Serri, C., Biondi, M., and Mayol, L. (2015) Surface modified natural zeolite as a carrier for sustained diclofenac release: A preliminary feasibility study. Colloids and Surfaces B: Biointerfaces, 130, 101–109.

de Gennaro, B., Mercurio, M., Cappelletti, P., Catalanotti, L., Daković, A., De Bonis, A., Grifa, C., Izzo, F., Kraković, M., Monetti, V., and others (2016) Use of surface modified natural zeolite (SMNZ) in pharmaceutical preparations. Part 2. A new approach for a fast functionalization of zeolite-rich carriers. Microporous and Mesoporous Materials, 235, 42–49.

de Gennaro, B., Izzo, F., Catalanotti, L., Langella, A., and Mercurio, M. (2017) Surface modified phillipsite as a potential carrier for NSAIDs release. Advanced Science Letters, 23, 5941–5943.

de Gennaro, M., Colella, C., Pansini, M., and Langella, A. (1992) Reconstruction of a natural zeolitization process through laboratory simulations. In Ninth International Zeolite Conference Vol. 2, pp. 207–214. Butterworth-Heinemann, Boston.

de Gennaro, M., Colella, C., Langella, A., and Cappelletti, P. (1995) Decay of Campanian ignimbrite stoneworks in some monuments of the Caserta area. Science and technology for cultural heritage, 4, 75–86.

de Gennaro, M., Langella, A., Cappelletti, P., and Colella, C. (1999) Hydrothermal conversion of trachytic glass to zeolite. 3. Monocationic model glasses. Clays and Clay Minerals, 47, 348–357.

de Gennaro, M., Calcaterra, D., Cappelletti, P., Langella, A., and Morra, V. (2000)

569 Building stone and related weathering in the architecture of the ancient city of
570 Naples. Journal of Cultural Heritage, 1, 399–414.
571 de Gennaro, R., Cappelletti, P., Cerri, G., de' Gennaro, M., Dondi, M., Guarini, G.,
572 Langella, A., and Naimo, D. (2003) Influence of zeolites on the sintering and
573 technological properties of porcelain stoneware tiles. Journal of the European
574 Ceramic Society, 23, 2237–2245.
575 de Gennaro, R., Cappelletti, P., Cerri, G., de' Gennaro, M., Dondi, M., and Langella, A.
576 (2004) Zeolitic tuffs as raw materials for lightweight aggregates. Applied Clay
577 Science, 25, 71–81.
578 de Gennaro, R., Cappelletti, P., Cerri, G., De'Gennaro, M., Dondi, M., and Langella, A.
579 (2005) Neapolitan Yellow Tuff as raw material for lightweight aggregates in
580 lightweight structural concrete production. Applied Clay Science, 28, 309–319.
581 de Gennaro, R., Cappelletti, P., Cerri, G., de' Gennaro, M., Dondi, M., Graziano, S.F.,
582 and Langella, A. (2007) Campanian Ignimbrite as raw material for lightweight
583 aggregates. Applied Clay Science, 37, 115–126.
584 de Gennaro, R., Langella, A., D'Amore, M., Dondi, M., Colella, A., Cappelletti, P.,
585 and De'Gennaro, M. (2008) Use of zeolite-rich rocks and waste materials for the
586 production of structural lightweight concretes. Applied Clay Science, 41, 61–72.
587 Dondi, M., Cappelletti, P., D'Amore, M., de Gennaro, R., Graziano, S.F., Langella, A.,
588 Raimondo, M., and Zanelli, C. (2016) Lightweight aggregates from waste
589 materials: Reappraisal of expansion behavior and prediction schemes for bloating.
590 Construction and Building Materials, 127, 394–409.
591 Esposito, S., Marocco, A., Dell'Agli, G., De Gennaro, B., and Pansini, M. (2015)

592 Relationships between the water content of zeolites and their cation population.
593 Microporous and Mesoporous Materials, 202, 36–43.
594 Fialips, C.I., Carey, J.W., and Bish, D.L. (2005) Hydration-dehydration behavior and
595 thermodynamics of chabazite. Geochimica et Cosmochimica Acta, 69, 2293–2308.
596 Foo, K.Y., and Hameed, B.H. (2010) Insights into the modeling of adsorption isotherm
597 systems. Chemical Engineering Journal.
598 Gabriele, G.A., and Ragsdell, K.M. (1977) The generalized reduced gradient method:
599 A reliable tool for optimal design. Journal of Engineering for Industry, 99, 394–
600 400.
601 Gatta, G.D., Cappelletti, P., de' Gennaro, B., Rotiroti, N., and Langella, A. (2015) New
602 data on Cu-exchanged phillipsite: a multi-methodological study. Physics and
603 Chemistry of Minerals, 42, 723–733.
604 Gondalia, R., Mashru, R., and Savaliya, P. (2010) Development and validation of
605 spectrophotometric methods for simultaneous estimation of ibuprofen and
606 paracetamol in soft gelatin capsule by simultaneous equation method.
607 International journal of chemtech research, 2, 1881–1885.
608 Hailu, S.L., Nair, B.U., Redi-Abshiro, M., DIaz, I., and Tessema, M. (2017)
609 Preparation and characterization of cationic surfactant modified zeolite adsorbent
610 material for adsorption of organic and inorganic industrial pollutants. Journal of
611 Environmental Chemical Engineering, 5, 3319–3329.
612 Higuchi, T. (1963) Mechanism of sustained-action medication. Theoretical analysis of
613 rate of release of solid drugs dispersed in solid matrices. Journal of
614 pharmaceutical sciences, 52, 1145–1149.

615 Hinz, C. (2001) Description of sorption data with isotherm equations. Geoderma, 99,
616 225–243.
617 Ho, Y.-S., Chiu, W.-T., and Wang, C.-C. (2005) Regression analysis for the sorption
618 isotherms of basic dyes on sugarcane dust. Bioresource Technology, 96, 1285–
619 1291.
620 Ho, Y.S. (2004) Citation review of Lagergren kinetic rate equation on adsorption
621 reactions. Scientometrics.
622 ——— (2006) Review of second-order models for adsorption systems. Journal of
623 Hazardous Materials, 136, 681–689.
624 Izzo, F., Mercurio, M., Aprea, P., Cappelletti, P., de Gennaro, B., Germinario, C., Grifa,
625 C., Pasquino, R., and Langella, A. (2017) Technological performance of Surface
626 Modified Natural Zeolite (SMNZ) for in vitro loading/release of ibuprofen
627 sodium salt: new insights on chabazite-rich tuff. In CONGRESSO SIMP-SGI-
628 SOGEI-AIV 2017 Geosciences: a tool in a changing world p. 221. Pisa.
629 Janićijević, J., Krajišnik, D., Čalija, B., Vasiljević, B.N., Dobričić, V., Daković, A.,
630 Antonijević, M.D., and Milić, J. (2015) Modified local diatomite as potential
631 functional drug carrier—A model study for diclofenac sodium. International
632 journal of pharmaceutics, 496, 466–474.
633 Joshi, R.S., Pawar, N.S., Katiyar, S.S., Zope, D.B., and Shinde, A.T. (2011)
634 Development and validation of UV spectrophotometric methods for simultaneous
635 estimation of Paracetamol and Ibuprofen in pure and tablet dosage form. Der
636 Pharmacia Sinica, 2, 164–171.
637 Karge, H.G. (2001) Characterization by IR spectroscopy. Verified Syntheses of

638 Zeolitic Materials. New York: John Wiley and Sons Inc, 69–71.
639 Krajišnik, D., Milojević, M., Malenović, A., Daković, A., Ibrić, S., Savić, S., Dondur,
640 V., Matijašević, S., Radulović, A., Daniels, R., and others (2010a) Cationic
641 surfactants-modified natural zeolites: improvement of the excipients functionality.
642 Drug Development and Industrial Pharmacy, 36, 1215–1224.
643 Krajišnik, D., Daković, A., Malenović, A., Milojević, M., Dondur, V., and Milić, J.
644 (2010b) Cationic surfactants-modified natural zeolites: potential excipients for
645 anti-inflammatory drugs. In Proceedings of the 3rd Croatian–Slovenian
646 Symposium on Zeolites, Trogir, Croatia pp. 23–26.
647 Krajišnik, D., Daković, A., Milojević, M., Malenović, A., Kragović, M., Bogdanović,
648 D.B., Dondur, V., and Milić, J. (2011) Properties of diclofenac sodium sorption
649 onto natural zeolite modified with cetylpyridinium chloride. Colloids and
650 Surfaces B: Biointerfaces, 83, 165–172.
651 Krajišnik, D., Daković, A., Malenović, A., Djekić, L., Kragović, M., Dobričić, V., and
652 Milić, J. (2013a) An investigation of diclofenac sodium release from
653 cetylpyridinium chloride-modified natural zeolite as a pharmaceutical excipient.
654 Microporous and Mesoporous Materials, 167, 94–101.
655 Krajišnik, D., Daković, A., Malenović, A., Milojević-Rakić, M., Dondur, V.,
656 Radulović, Ž., and Milić, J. (2013b) Investigation of adsorption and release of
657 diclofenac sodium by modified zeolites composites. Applied Clay Science, 83–84,
658 322–326.
659 Krajišnik, D., Daković, A., Malenović, A., Kragović, M., and Milić, J. (2015)
660 Ibuprofen sorption and release by modified natural zeolites as prospective drug

carriers. (G. Christidis, Ed.)Clay Minerals, 50, 11–22.

Kranz, R.L., Bish, D.L., and Blacic, J.D. (1989) Hydration and dehydration of Zeolitic Tuff from Yucca Mountain, Nevada. Geophysical Research Letters, 16, 1113–1116.

Langella, A., De Simone, P., Calcaterra, D., Cappelletti, P., and De'Gennaro, M. (2002) Evidence of the relationship occurring between zeolitization and lithification in the yellow facies of Campanian Ignimbrite (southern Italy). Studies in Surface Science and Catalysis, 142, 1775–1782.

Langella, A., Pansini, M., Cerri, G., Cappelletti, P., and De'Gennaro, M. (2003) Thermal behavior of natural and cation-exchanged clinoptilolite from Sardinia (Italy). Clays and Clay Minerals, 51, 625–633.

Langella, A., Bish, D.L., Cappelletti, P., Cerri, G., Colella, A., de Gennaro, R., Graziano, S.F., Perrotta, A., Scarpati, C., and de Gennaro, M. (2013) New insights into the mineralogical facies distribution of Campanian Ignimbrite, a relevant Italian industrial material. Applied Clay Science, 72, 55–73.

Langmuir, I. (1916) the Constitution and Fundamental Properties of Solids and Liquids. Part I. Solids. Journal of the American Chemical Society, 252, 2221–2295.

Larsson, D.G.J. (2014) Pollution from drug manufacturing: review and perspectives. Philosophical transactions of the Royal Society of London. Series B, Biological sciences, 369, 20130571-.

Li, Z., and Bowman, R.S. (1997) Counterion effects on the sorption of cationic surfactant and chromate on natural clinoptilolite. Environmental Science and Technology, 31, 2407–2412.

Li, Z., and Bowman, R.S. (1998) Sorption of chromate and PCE by surfactant-modified clay minerals. Environmental Engineering Science, 15, 237–245.

Li, Z., and Bowman, R.S. (2001) Regeneration of surfactant-modified zeolite after saturation with chromate and perchloroethylene. Water Research, 35, 322–326.

Li, Z., Anghel, I., and Bowman, R.S. (1998) Sorption of Oxyanions By Surfactant-Modified Zeolite. Journal of Dispersion Science and Technology, 19, 843–857.

Li, Z., Jones, H.K., Bowman, R.S., and Helferich, R. (1999) Enhanced reduction of chromate and PCE by pelletized surfactant-modified zeolite/zerovalent iron. Environmental Science and Technology, 33, 4326–4330.

Limousin, G., Gaudet, J.P., Charlet, L., Szenknect, S., Barthès, V., and Krimissa, M. (2007) Sorption isotherms: A review on physical bases, modeling and measurement. Applied Geochemistry.

Lin, J., and Wang, L. (2009) Comparison between linear and non-linear forms of pseudo-first-order and pseudo-second-order adsorption kinetic models for the removal of methylene blue by activated carbon. Frontiers of Environmental Science & Engineering in China, 3, 320–324.

Markandeya, S.P., and Kisku, G.C. (2015) Linear and Non-Linear Kinetic Modeling for Adsorption of Disperse Dye in Batch Process. Research Journal of Environmental Toxicology, 9, 320–331.

Marković, M., Daković, A., Krajišnik, D., Kragović, M., Milić, J., Langella, A., de Gennaro, B., Cappelletti, P., and Mercurio, M. (2016) Evaluation of the surfactant/phillipsite composites as carriers for diclofenac sodium. Journal of Molecular Liquids, 222, 711–716.

Marković, M., Daković, A., Rottinghaus, G.E., Kragović, M., Petković, A., Krajišnik, D., Milić, J., Mercurio, M., and de Gennaro, B. (2017) Adsorption of the mycotoxin zearalenone by clinoptilolite and phillipsite zeolites treated with cetylpyridinium surfactant. Colloids and Surfaces B: Biointerfaces, 151, 324–332.

Mercurio, M., Mercurio, V., de'Gennaro, B., de'Gennaro, M., Grifa, C., Langella, A., and Morra, V. (2010) Natural zeolites and white wines from Campania region (Southern Italy): a new contribution for solving some oenological problems. Periodico di Mineralogia, 79, 95–112.

Mercurio, M., Langella, A., Cappelletti, P., de Gennaro, B., Monetti, V., and de Gennaro, M. (2012) May the use of Italian volcanic zeolite-rich tuffs as additives in animal diet represent a risk for the human health. Period Mineral, 81, 393–407.

Mercurio, M., Grilli, E., Odierna, P., Morra, V., Prohaska, T., Coppola, E., Grifa, C., Buondonno, A., and Langella, A. (2014) A "Geo-Pedo-Fingerprint" (GPF) as a tracer to detect univocal parent material-to-wine production chain in high quality vineyard districts, Campi Flegrei (Southern Italy). Geoderma, 230–231, 64–78.

Mercurio, M., Bish, D.L., Cappelletti, P., Gennaro, B. de, Gennaro, M. de, Grifa, C., Izzo, F., Mercurio, V., Morra, V., and Langella, A. (2016a) The combined use of steam-treated bentonites and natural zeolites in the oenological refining process. Mineralogical Magazine, 80, 347–362.

Mercurio, M., Cappelletti, P., De Gennaro, B., De Gennaro, M., Bovera, F., Iannaccone, F., Grifa, C., Langella, A., Monetti, V., and Esposito, L. (2016b) The effect of digestive activity of pig gastro-intestinal tract on zeolite-rich rocks: An in vitro study. Microporous and Mesoporous Materials, 225, 133–136.

730 Morra, V., Calcaterra, D., Cappelletti, P., Colella, A., Fedele, L., De'Gennaro, R.,
731 Langella, A., Mercurio, M., and De'Gennaro, M. (2010) Urban geology:
732 relationships between geological setting and architectural heritage of the
733 Neapolitan area. Eds.) Marco Beltrando, Angelo Peccerillo, Massimo Mattei,
734 Sandro Conticelli, and Carlo Doglioni, Journal of the Virtual Explorer, 36, 1–60.
735 Mozgawa, W., Król, M., and Barczyk, K. (2011) FT-IR studies of zeolites from
736 different structural groups. CHEMIK nauka-technika-rynek, 1, 667–674.
737 Oh, S., Shin, W.S., and Kim, H.T. (2016) Effects of pH, dissolved organic matter, and
738 salinity on ibuprofen sorption on sediment. Environmental Science and Pollution
739 Research, 23, 22882–22889.
740 Pansini, M., Colella, C., Caputo, D., De'Gennaro, M., and Langella, A. (1996)
741 Evaluation of phillipsite as cation exchanger in lead removal from water.
742 Microporous Materials.
743 Pasquino, R., Di Domenico, M., Izzo, F., Gaudino, D., Vanzanella, V., Grizzuti, N.,
744 and de Gennaro, B. (2016) Rheology-sensitive response of zeolite-supported anti-
745 inflammatory drug systems. Colloids and Surfaces B: Biointerfaces, 146, 938–944.
746 Płuciennik-Koropczuk, E. (2014) Non-Steroid Anti-Infflamatory Drugs in Municipal
747 Wastewater and Surface Waters/ Niesteroidowe Leki Przeciwzaplane W Ściekach
748 Mieskich I Wodach Powierzchniowych. Civil And Environmental Engineering
749 Reports, 14.
750 Sena, M.M., Freitas, C.B., Silva, L.C., Pérez, C.N., and de Paula, Y.O. (2007)
751 Determinação espectrofotométrica simultânea de paracetamol e ibuprofeno em
752 formulações farmacêuticas usando calibração multivariada. Química Nova, 30,

753 75–79.
754 Serri, C., De Gennaro, B., Catalanotti, L., Cappelletti, P., Langella, A., Mercurio, M.,
755 Mayol, L., and Biondi, M. (2016) Surfactant-modified phillipsite and chabazite as
756 novel excipients for pharmaceutical applications? Microporous and Mesoporous
757 Materials, 224, 143–148.
758 Serri, C., de Gennaro, B., Quagliariello, V., Iaffaioli, R.V., De Rosa, G., Catalanotti, L.,
759 Biondi, M., and Mayol, L. (2017) Surface modified zeolite-based granulates for
760 the sustained release of diclofenac sodium. European Journal of Pharmaceutical
761 Sciences, 99, 202–208.
762 Sips, R. (1948) Combined form of Langmuir and Freundlich equations. J. Chem. Phys,
763 16, 490–495.
764 Spiess, A.-N., and Neumeyer, N. (2010) An evaluation of R2 as an inadequate measure
765 for nonlinear models in pharmacological and biochemical research: a Monte Carlo
766 approach. BMC pharmacology, 10, 6.
767 Sullivan, E.J., Hunter, D.B., and Bowman, R.S. (1997) Topological and thermal
768 properties of surfactant-modified clinoptilolite studied by tapping-mode atomic
769 force microscopy and high-resolution thermogravimetric analysis. Clays and Clay
770 Minerals, 45, 42–53.
771 Tan, D., Yuan, P., Annabi-Bergaya, F., Yu, H., Liu, D., Liu, H., and He, H. (2013)
772 Natural halloysite nanotubes as mesoporous carriers for the loading of ibuprofen.
773 Microporous and Mesoporous Materials, 179, 89–98.
774 Toth, J. (1971) State equations of the solid-gas interface layers. Acta Chim Acad Sci
775 Hungar, 69, 311–328.

776 USP-NF (2002) The United States Pharmacopeia and the National Formulary, 25th ed.
777 United States Pharmacopeial Convention Inc., Rockville, MD, USA.
778 ——— (2003) The United States Pharmacopeia and the National Formulary, 26th ed.
779 United States Pharmacopeial Convention Inc., Rockville, MD, USA.
780 Wang, S., and Peng, Y. (2010) Natural zeolites as effective adsorbents in water and
781 wastewater treatment. Chemical Engineering Journal, 156, 11–24.
782 Wray, P.S., Clarke, G.S., and Kazarian, S.G. (2011) Application of FTIR spectroscopic
783 imaging to study the effects of modifying the pH microenvironment on the
784 dissolution of ibuprofen from HPMC matrices. Journal of pharmaceutical sciences,
785 100, 4745–4755.
786 Yadav, G., Bansal, M., Thakur, N., and Khare, P. (2013) Multilayer Tablets and Their
787 Drug Release Kinetic Models for Oral Controlled Drug Delivery System. Middle-
788 East Journal of Scientific Research, 16, 782–795.
789
790

791
792 FIGURE CAPTIONS

793

794 Figure 1 - Physico-chemical and thermal properties of IBU
795
796 Figure 2 - Physico-chemical and thermal properties of surfactants
797
798 Figure 3 - FTIR spectra of starting materials (PHI_SAV), SMNZ (PCC), IBU-loaded
799 SMNZ (PCC+IBU)
800
801 Figure 4 - Thermal properties of starting materials by TG/DSC coupled with FTIR-
802 EGA
803
804 Figure 5 - Isotherms: A-Langmuir; B-Sips; C-Toth
805
806 Figure 6 - Kinetic loading curves: A- Pseudo-first order, B- Pseudo-second order
807
808 Figure 7 - Kinetic release curves: A- First-order, B- Weibull, C- First order (%), D-
809 Weibull (%).
810

This is a preprint, the final version is subject to change, of the American Mineralogist (MSA)
Cite as Authors (Year) Title. American Mineralogist, in press.
DOI: https://doi.org/10.2138/am-2018-6328

Revision 2

Table 1 – FTIR data

PHI SAV	PCC	PBC	PHC	PHB	PCC+IBU	PBC+IBU	PHC+IBU	PHB+IBU	Tentative vibrational assignments	Chemical phase
3419 w	3422 w	3436 w	3425 w	3427 w	3426 w	3434 w	3422 w	3425 w	O-H stretching	water
	2958 sh	2959 sh	2958 sh	2959 sh	2955 vw	2960 sh	2954 sh	2954 sh	C–H stretching	Surfactant/IBU
	2917 w	2923 vw	2923 vw	2923 vw	2921 w	2924 vw	2920 w	2922 w	C–H stretching	Surfactant/IBU
	2850 w	2853 vw	2852 vw	2852 vw	2851 w	2853 vw	2851 w	2852 w	C–H stretching	Surfactant/IBU
1638 w	1635 w	1639 w	1638 w	1639 w	1635 w	1638 w	1638 w	1638 w	O-H bending	water
					1572 vw	1573 sh	1580 sh	1582 sh	Asymmetric stretching in carboxylate ion	IBU
	1489 vw	1481 vw	1489 sh	1489 sh	1489 vw	1481 vw	1489 sh	1489 sh	C−H bending	Surfactant/IBU
	1469 vw	1466 vw	1470 vw	1470 vw	1466 vw	1466 vw	1469 vw	1467 vw	C−H bending	Surfactant/IBU
1456 vw									C-O asymmetric stretching	Calcite
					1382 vw	1379 vw	1376 vw	1381 vw	Symmetric stretching in carboxylate ion	IBU
1000 vs	995 vs	992 vs	995 vs	992 vs	989 vs	992 vs	991 vs	989 vs	T-O asymmetric stretching	silicates
780 w	774 w	781 w	779 w	777 w	775 w	781 w	776 w	778 w	T-O-T asymmetric stretching	silicates
719 w	717 w	723 w	720 w	719 w	719 w	724 w	720 w	719 w	T-O-T symmetric stretching	silicates
633 sh	633 sh	633 sh	632 sh	632 sh	633 sh	633 sh	633 sh	633 sh	T-O-T bending	silicates
597 w	596 w	597 w	597 w	599 w	595 w	598 w	596 w	598 w	T-O-T bending	silicates
516 vw	515 vw	519 vw	517 vw	516 vw	514 vw	517 vw	519 vw	516 vw	T-O-T bending	silicates
426 w	427 w	427 w	424 w	429 w	423 w	428 w	427 w	421 w	T-O-T bending	Silicates

Legend: w, weak; vw, very weak; sh, shoulder; s, strong; vs, very strong; T, tetrahedral cation (Si or Al).

This is a preprint, the final version is subject to change, of the American Mineralogist (MSA)
Cite as Authors (Year) Title. American Mineralogist, in press.
DOI: https://doi.org/10.2138/am-2018-6328

Revision 2

Table 2 –Thermal Analysis (TG-DTG-DSC and FTIR-EGA) data

Samples	T < 200 °C				200 °C < T < 1050 °C				L.O.I (%)	R.M. (%)
	ΔW(%)	DTG (°C)	DSC[(a)](°C)	EGA	ΔW(%)	DTG (°C)	DSC[(b)](°C)	EGA		
PCC	6.3	157	131	H_2O	9.0	230-499-665	246-333-502-672[(a)]-929	$CO_2 + CH_3 + CH_2 + H_2O^{tr} + CO^{tr}$	15.3	84.7
PCC+IBU	6.6	162	118	H_2O	11.0	206-488-655	223-339-498-686[(a)]-939	$CO_2 + CH_3 + CH_2 + H_2O^{tr} + CO^{tr}$	17.5	82.5
PBC	6.1	153	164	H_2O	7.1	212-384-525-659	226[(a)]-275-386-528-644[(a)]-929	$CO_2 + CH_3 + CH_2 + H_2O^{tr} + CO^{tr}$	13.3	86.8
PBC+IBU	6.8	150	167	H_2O	7.7	211-384-514-646	230[(a)]-277-388-519-646[(a)]-932	$CO_2 + CH_3 + CH_2 + H_2O^{tr} + CO^{tr}$	14.5	85.5
PHC	6.7	144	157	H_2O	7.2	235-517-646	225-299-389-495-649[(a)]-916	$CO_2 + CH_3 + CH_2 + H_2O^{tr} + CO^{tr}$	14.0	86.0
PHC+IBU	7.6	154	151	H_2O	8.5	216-513-648	286-380-481-645[(a)]-943	$CO_2 + CH_3 + CH_2 + H_2O^{tr} + CO^{tr}$	16.1	83.9
PHB	6.9	146	144	H_2O	6.8	381-504-664	283-369-503-651[(a)]-930	$CO_2 + CH_3 + CH_2 + H_2O^{tr} + CO^{tr}$	13.7	86.3
PHB+IBU	6.8	146	153	H_2O	9.1	226-385-499-665	234-296-388-476-658[(a)]-943	$CO_2 + CH_3 + CH_2 + H_2O^{tr} + CO^{tr}$	15.9	84.1

LEGEND:

[(a)]= Endothermic

[(b)]= Exothermic

L.O.I. = loss on ignition

R.M. = residual mass

ΔW = weight loss (by TG)

[(tr)]= traces

This is a preprint, the final version is subject to change, of the American Mineralogist (MSA)
Cite as Authors (Year) Title. American Mineralogist, in press.
DOI: https://doi.org/10.2138/am-2018-6328

Revision 1

Table 3 - Isotherm parameters

Samples	Mathematical model	Parameters				Goodness-of-fit		
		K (L/mg)	n	S_m (mg/g)	S_m (mEq/g)	R^2	AIC	BIC
PCC	Langmuir	0.032		22.0 ± 0.6	0.096	0.970	27.1	27.0
	Sips	0.026	2.91	20.4 ± 0.25	0.089	0.987	23.1	22.9
	Toth	0.014	3.85	20.4 ± 0.2	0.089	0.987	23.1	22.9
PBC	Langmuir	0.039		21.9 ± 0.5	0.096	0.981	24.2	24.1
	Sips	0.040	1.06	21.7 ± 0.4	0.095	0.981	26.1	26.0
	Toth	0.033	1.16	21.4 ± 0.4	0.094	0.982	26.0	25.9
PHC	Langmuir	0.018		26.1 ± 0.5	0.114	0.989	22.2	22.1
	Sips	0.018	1.38	24.6 ± 0.3	0.108	0.993	21.1	21.0
	Toth	0.011	1.62	24.4 ± 0.2	0.107	0.993	20.5	20.3
PHB	Langmuir	0.006		36.2 ± 1.6	0.158	0.981	29.6	29.5
	Sips	0.008	1.54	31.0 ± 0.9	0.136	0.991	26.3	26.2
	Toth	0.004	3.83	28.8 ± 0.3	0.126	0.995	21.7	21.6

Table 4 - IBU Loading kinetic runs parameters

Samples	Mathematical model	Parameters				Goodness-of-fit		
		K_1 (min^{-1})	K_2 ($g \cdot mg^{-1} \cdot min^{-1}$)	Q_0 (mg/g)	Q_0 (mEq/g)	R^2	AIC	BIC
PCC	Pseudo-first order	0.333		18.9 ± 1.1	0.083	0.983	27.9	28.7
	Pseudo-second order		0.041	19.3 ± 0.5	0.085	0.987	24.9	25.7
PBC	Pseudo-first order	0.073		19.2 ± 0.7	0.084	0.975	38.9	37.7
	Pseudo-second order		0.005	20.9 ± 0.5	0.091	0.979	35.2	36.0
PHC	Pseudo-first order	0.620		26.3 ± 0.4	0.115	0.996	19.3	20.1
	Pseudo-second order		0.155	26.4 ± 0.4	0.116	0.996	19.3	20.1
PHB	Pseudo-first order	0.005		27.0 ± 1.7	0.118	0.967	43.0	43.8
	Pseudo-second order		0.021	27.9 ± 0.9	0.122	0.988	31.7	32.5

Table 5 - IBU Release kinetic runs parameters

Samples	Mathematical model	Parameters					Goodness-of-fit		
		K_1 (min^{-1})	a (min)	b	M_0 (mg/g)	M_0 (%)	R^2	AIC	BIC
PCC	First-order	0.033			18.4 ± 0.9	95.45	0.995	14.9	15.7
	Weibull		31.61	1.31	18.3 ± 0.6	94.71	0.997	9.7	10.9
PBC	First-order	0.036			19.0 ± 0.7	98.44	0.990	22.6	23.4
	Weibull		30.53	1.89	18.8 ± 0.2	97.26	0.999	-0.5	0.7
PHC	First-order	0.036			25.5 ± 1.0	96.54	0.995	21.5	22.3
	Weibull		30.08	1.51	25.3 ± 0.5	95.71	0.999	2.4	3.6
PHB	First-order	0.033			25.9 ± 1.2	92.83	0.988	31.4	32.2
	Weibull		33.19	1.68	25.6 ± 0.6	91.58	0.998	13.1	13.3

This is a preprint, the final version is subject to change, of the American Mineralogist (MSA)
Cite as Authors (Year) Title. American Mineralogist, in press.
DOI: https://doi.org/10.2138/am-2018-6328

Figure 1

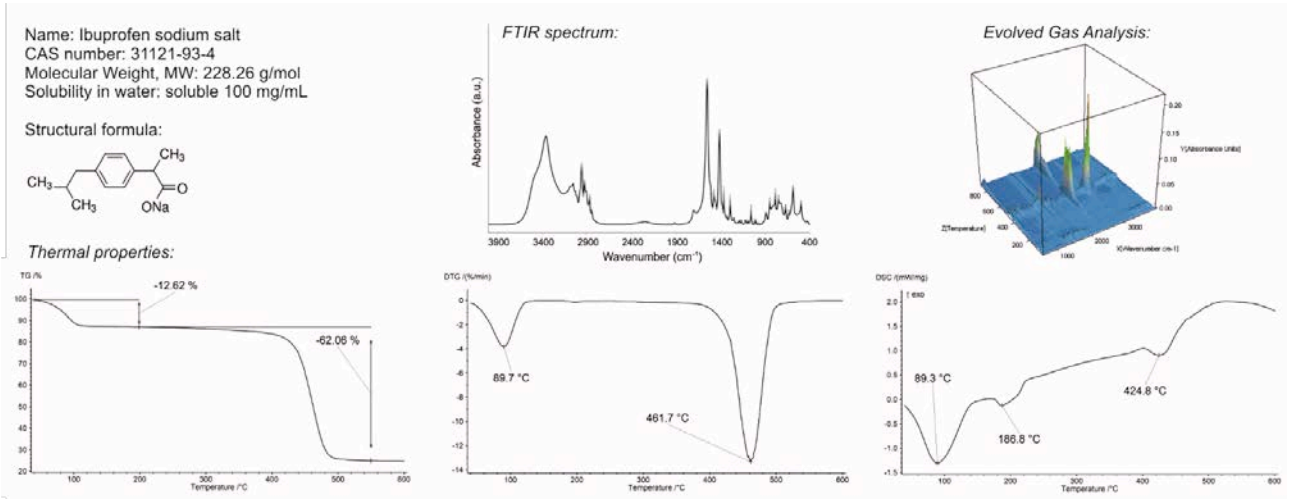

This is a preprint, the final version is subject to change, of the American Mineralogist (MSA)
Cite as Authors (Year) Title. American Mineralogist, in press.
DOI: https://doi.org/10.2138/am-2018-6328

Figure 2

Name: Cetylpyridinum chloride
CAS number: 123-03-5
Molecular Weight, MW: 358 g/mol
Critical Micelle Concentration, CMC: 0.9 mmol/L

Structural formula:

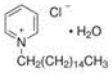

Thermal properties:

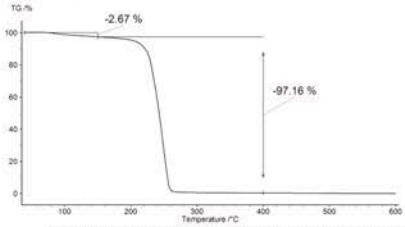

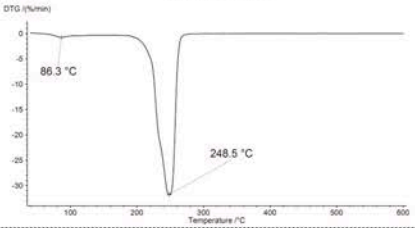

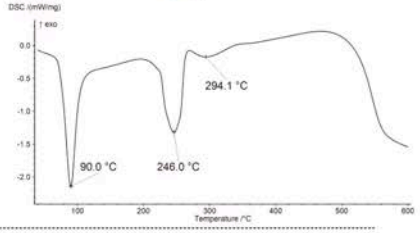

FTIR spectrum:

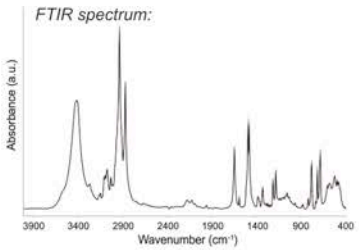

Evolved Gas Analysis:

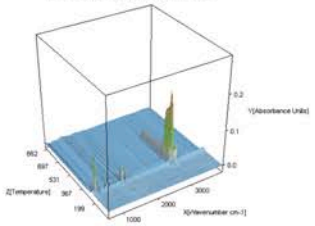

Name: Benzalkonium chloride
CAS number: 63449-41-2
Molecular Weight, MW: 354 g/mol
Critical Micelle Concentration, CMC: 5 mmol/L

Structural formula:

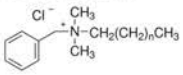

Thermal properties:

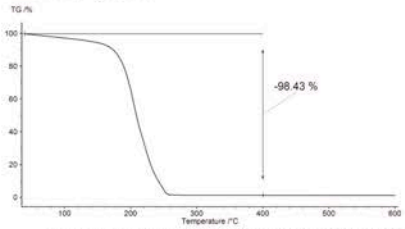

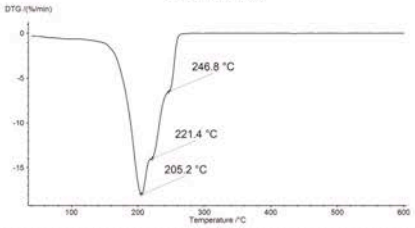

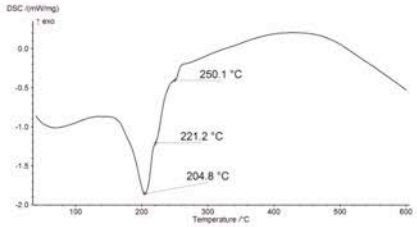

FTIR spectrum:

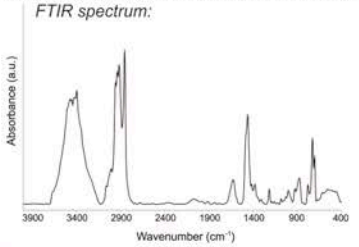

Evolved Gas Analysis:

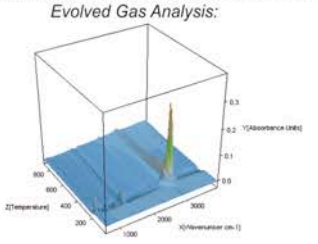

Name:Hexadecyltrimethylammonium chloride
CAS number: 112-02-7
Molecular Weight, MW: 320 g/mol
Critical Micelle Concentration, CMC: 1.3 mmol/L

Structural formula:

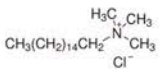

Thermal properties:

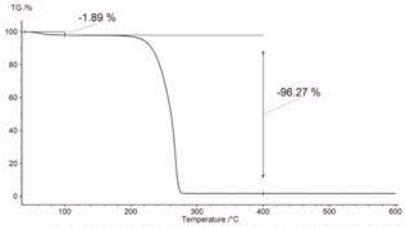

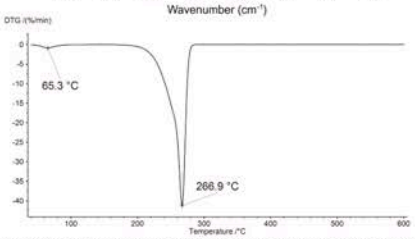

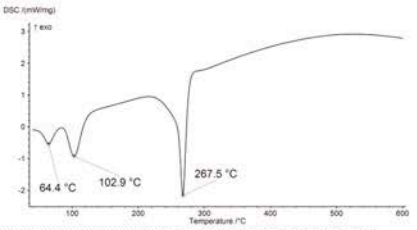

FTIR spectrum:

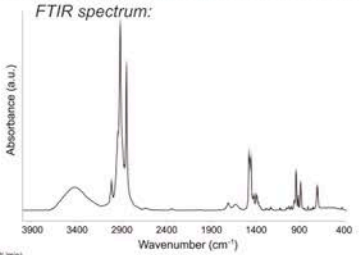

Evolved Gas Analysis:

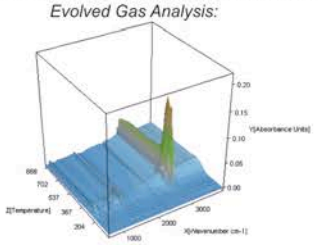

Name: Hexadecyltrimethylammonium bromide
CAS number: 57-09-0
Molecular Weight, MW: 364.46 g/mol
Critical Micelle Concentration, CMC: 0.9 mmol/L

Structural formula:

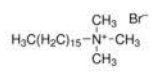

Thermal properties:

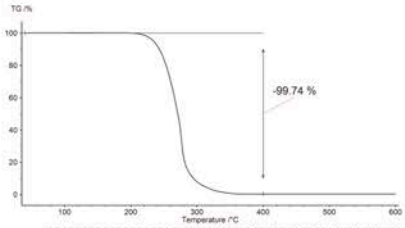

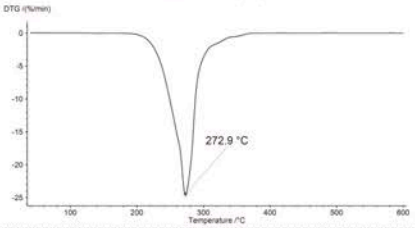

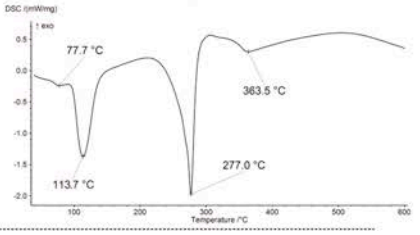

FTIR spectrum:

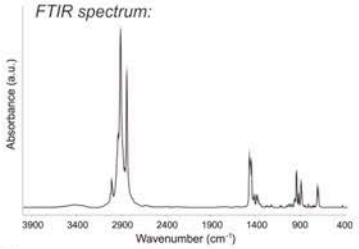

Evolved Gas Analysis:

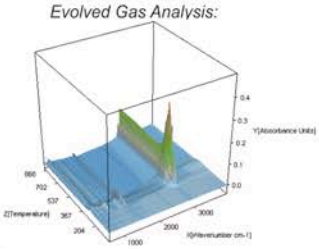

This is a preprint, the final version is subject to change, of the American Mineralogist (MSA)
Cite as Authors (Year) Title. American Mineralogist, in press.
DOI: https://doi.org/10.2138/am-2018-6328

Figure 3

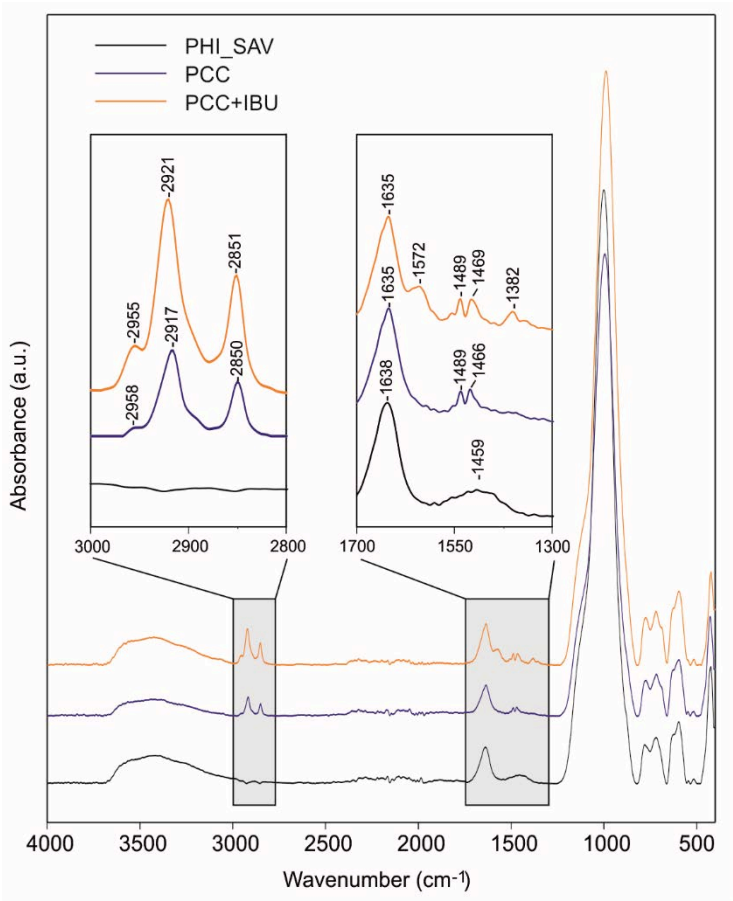

This is a preprint, the final version is subject to change, of the American Mineralogist (MSA)
Cite as Authors (Year) Title. American Mineralogist, in press.
DOI: https://doi.org/10.2138/am-2018-6328

Figure 4

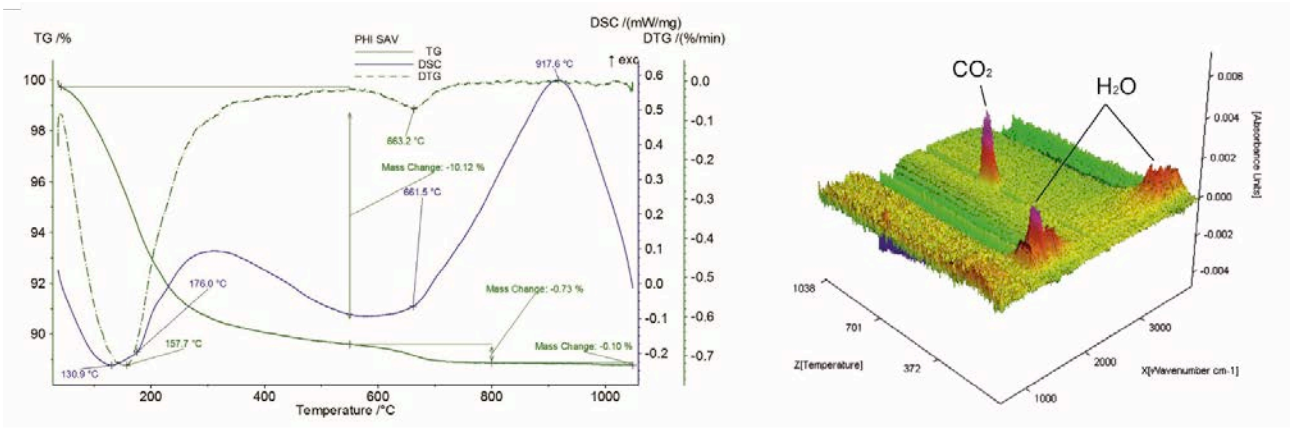

This is a preprint, the final version is subject to change, of the American Mineralogist (MSA)
Cite as Authors (Year) Title. American Mineralogist, in press.
DOI: https://doi.org/10.2138/am-2018-6328

Figure 5

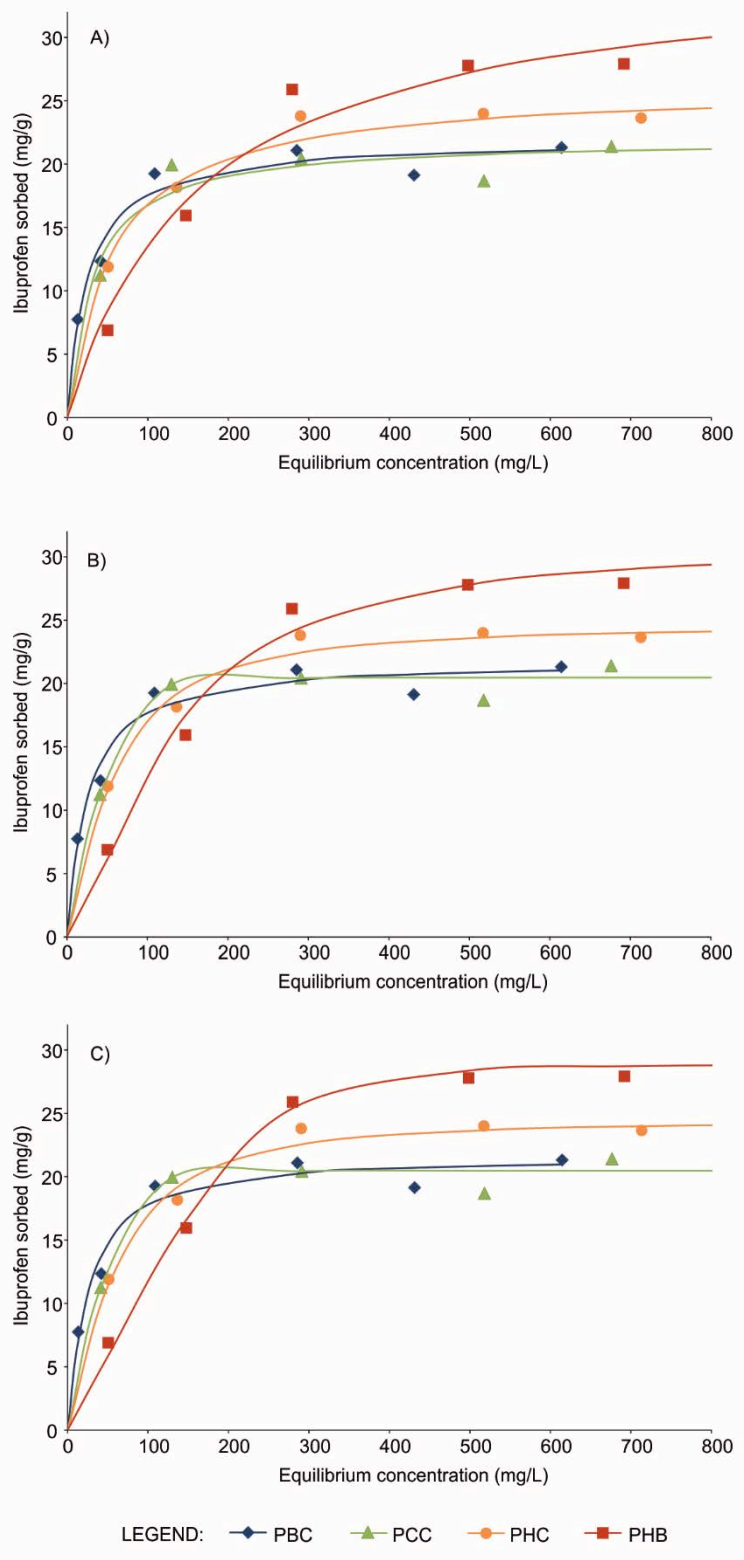

This is a preprint, the final version is subject to change, of the American Mineralogist (MSA)
Cite as Authors (Year) Title. American Mineralogist, in press.
DOI: https://doi.org/10.2138/am-2018-6328

Figure 6

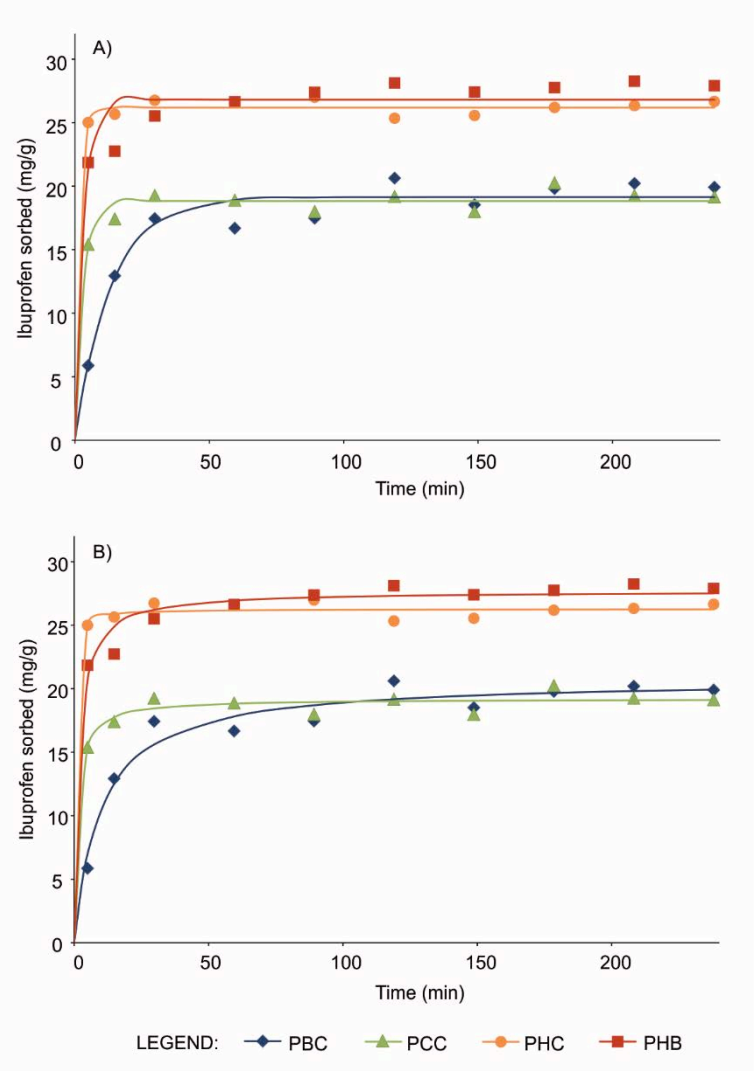

This is a preprint, the final version is subject to change, of the American Mineralogist (MSA)
Cite as Authors (Year) Title. American Mineralogist, in press.
DOI: https://doi.org/10.2138/am-2018-6328

Figure 7